Available online at www.sciencedirect.com

SCIENCE DIRECT®

Electrochimica Acta 49 (2004) 821–828

ELECTROCHIMICA Acta

www.elsevier.com/locate/electacta

Development and characterization of a silicon-based micro direct methanol fuel cell

G.Q. Lu [a], C.Y. Wang [a,*], T.J. Yen [b], X. Zhang [b]

[a] *Department of Mechanical and Nuclear Engineering, Electrochemical Engine Center (ECEC),*
Pennsylvania State University, University Park, PA 16802, USA
[b] *Department of Mechanical and Aerospace Engineering, University of California at Los Angeles,*
420 Westwood Plaza, Los Angeles, CA 90095, USA

Received 14 July 2003; received in revised form 8 September 2003; accepted 26 September 2003

Abstract

A silicon-based micro direct methanol fuel cell (μDMFC) for portable applications has been developed and its electrochemical characterization carried out in this study. Anode and cathode flowfields with channel and rib width of 750 μm and channel depth of 400 μm were fabricated on Si wafers using the microelectromechanical system (MEMS) technology. A membrane-electrode assembly (MEA) was specially fabricated to mitigate methanol crossover. This MEA features a modified anode backing structure in which a compact microporous layer is added to create an additional barrier to methanol transport thereby reducing the rate of methanol crossing over the polymer membrane. The cell with the active area of 1.625 cm^2 was assembled by sandwiching the MEA between two micro-fabricated Si wafers. Extensive cell polarization testing demonstrated a maximum power density of 50 $\mathrm{mW/cm}^2$ using 2 M methanol feed at 60 °C. When the cell was operated at room temperature, the maximum power density was shown to be about 16 $\mathrm{mW/cm}^2$ with both 2 and 4 M methanol feed. It was further found that the present μDMFC still produced reasonable performance under 8 M methanol solution at room temperature.

Keywords: DMFC; Methanol crossover; Micro fuel cell; MEMS

1. Introduction

Micro-power sources are a key technology in future integrated micro-systems that enable sensing, computing, actuation, control, and communication on a single chip. Due to such advantages as high energy-conversion efficiency, easy storage of liquid fuel, ambient temperature operation, and simple construction, the direct methanol fuel cell (DMFC) has received much attention as a leading candidate for portable power of the future [1,2]. Fundamentals of the DMFC system have been studied extensively [3–7].

Thanks to the integrated-circuit (IC) fabrication technology, micro-channel patterns of DMFC bipolar plates into which reactants are fed can be featured on the silicon wafer with high resolution and good repeatability. Kelley et al. [8] reported a 0.25 cm^2 micro DMFC (μDMFC) using Si wafer as the substrate. The anode catalyst in their micro DMFC was prepared by coelectrodepositing a Pt–Ru alloy onto a carbon coated Si wafer. Using 0.5 M methanol solution, the micro DMFC was tested and yielded an output current density very close to that of large-scale DMFC. In a subsequent paper [9], they reported that a prototype cell (12 mm^3 in volume) micro-fabricated on Si substrates and featuring electrodeposition of Pt–Ru as the anode catalyst successfully demonstrated a lowering of catalyst loading to 0.25 $\mathrm{mg/cm}^2$ without loss of performance. Lee et al. [10] reported a micro fuel cell design in which a planar array of cells are connected in series in a “flip-flop” configuration. It was suggested that this method was particularly favorable for miniature fuel cells and suited for prototyping using a variety of etch and deposition techniques on Si wafers adopted from micro-fabrication. The peak power in a four-cell silicon assembly was reported to reach 40 $\mathrm{mW/cm}^2$ using hydrogen and oxygen as fuel and oxidizer.

---

* Corresponding author. Tel.: +1-814-863-4762;
fax: +1-814-863-4848.
E-mail address: cxw31@psu.edu (C.Y. Wang).

0013-4686/$ – see front matter © 2003 Elsevier Ltd. All rights reserved.
doi:10.1016/j.electacta.2003.09.036

Maynard and Meyers [11] proposed a conceptual design for a miniaturized proton exchange membrane methanol-based fuel cell for powering 0.5–20 W portable telecommunication and computing devices. Their system was implemented on a Si substrate to leverage advanced Si processing and micro-electromechanical system (MEMS) technology. Heinzel et al. [12] demonstrated a prototype miniature fuel cell stack to power a laptop computer using hydrogen and air as reactants running at ambient pressure and temperature. Most recently, Yu et al. [13] fabricated a miniature twin-fuel-cell connected in series by sandwiching two membrane-electrode assemblies between two Si micro-machined plates. Pavio et al. [14] instead explored low-temperature co-fired ceramic (LTCC) material as an alternative for the bipolar plates of micro fuel cell systems. A DMFC prototype, packaged using LTCC, was reported in their paper [14].

In portable fuel cells, water and gas management represents a critical issue to enhancement of cell performance and sustained cell operation for an extended period of time. Blum et al. [15] discussed overall water balance between the cell's net production rate and water loss through an air-breathing cathode. It was recognized that a water-neutral condition occurs when the water molecules lost per molecule of methanol consumed by the cell reaction approaches two, a stoichiometric value of the net water production per mole of methanol. Under this water-neutral condition, there is neither need to carry water in the fuel tank of such a micro DMFC, nor dryout of the cell. Recently, Lu and Wang [16] presented a photographic study of bubble dynamics on the anode side and liquid water flooding on the cathode side, thereby providing a basic understanding of gas and water management requirements in DMFC and hence aiding a judicious selection of suitable materials for anode and cathode backing layers.

In the present work, a micro DMFC is fabricated on Si wafers using micro-electronic fabrication technology and assembled along with novel MEA that has been developed previously to resist methanol crossover. The micro DMFC is subsequently tested in a wide range of operating conditions where the methanol feed concentration varies from 1 to 8 M and the cell temperature from the ambient to 60 °C. The focus of this work is placed upon demonstrating acceptable micro DMFC performance with concentrated methanol solution. This strategy of practical importance aims to substantially increase the energy density of the entire system including the fuel cell and fuel tank and hence extend its run time.

2. Experimental

As shown in Fig. 1, a DMFC consists of two plates, one for the anode and the other for the cathode, and a MEA in between. The two plates with flow channels machined in are micro-fabricated from the Si wafer.

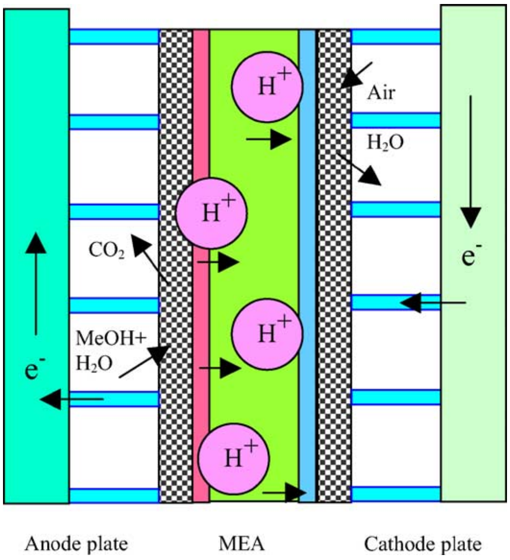

Fig. 1. Schematic of a direct methanol fuel cell (DMFC).

2.1. Fabrication of silicon wafer

The fabrication process is illustrated in Fig. 2. A pair of 500 ± 20 μm Si wafers were employed here. First, a 10 μm thick negative photoresist was transferred on the front-side of the wafer as an etching mask, and then deep reactive ion etching (DRIE) was applied to anisotropically inscribe fluid channels into the Si wafer with a depth of 400 μm. Both the flow channel and the rib separating two neighboring channels were 750 μm wide, with the channel length of 12.75 mm. There were a total of nine channels with serpentine flowfield, forming a cell effective area of approximately 1.625 cm^2. To fashion the fuel feeding holes, double-sided alignment photolithography was conducted to pattern the backside of wafers with the accuracy better than 10 μm. Another DRIE followed to fabricate through-hole

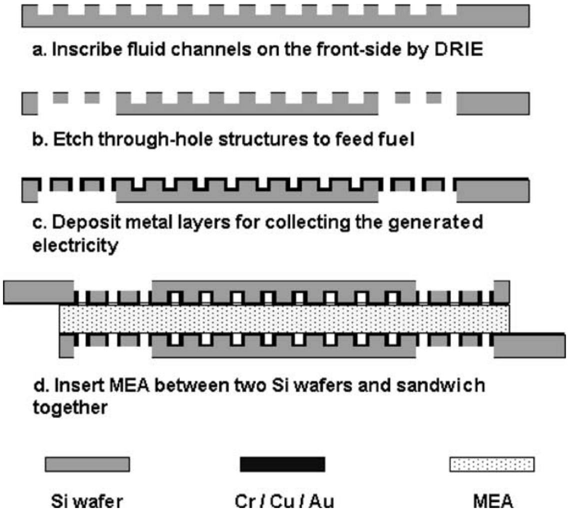

Fig. 2. Fabrication process flow of the μDMFC.

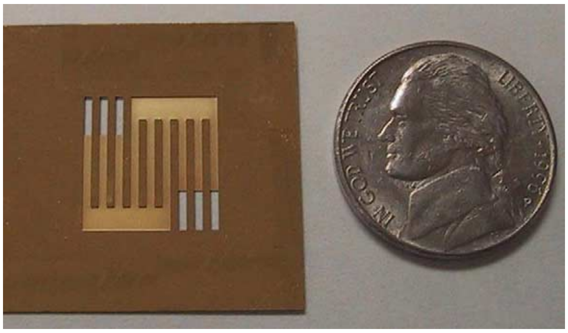

Fig. 3. Picture of a silicon wafer with flow channels.

structures, allowing methanol fuel to flow in and out. In order to collect current and to minimize contact resistance between the MEA and the Si wafer, Cr/Cu/Au (with thickness of 0.01/3/0.5 μm) were deposited on the front-side of each wafer by electron beam evaporation. Fig. 3 shows a picture of the silicon wafer with fabricated flow channel pattern.

2.2. MEA preparation

Both backing layers of anode and cathode were 20 wt.% FEP wet-proofed carbon paper (Toray 090, E-Tek) of 0.26 mm in thickness. Our approach to make a more methanol resistant MEA is to modify the anode structure by providing additional diffusion barriers to methanol transport in the backing layer rather than using an alternative, novel membrane. Details of this approach have been elaborated in [16,17] and the reader is referred to those papers for further information. A mixture solution containing Vulcan XC72R carbon black and 40 wt.% Teflon (TFE 30, Dupont) was coated on the carbon paper using a gap-adjustable knife-blade to form a microporous layer. Subsequently, the coated carbon paper was dried at 100 °C for 30 min and at 360 °C for 15 min in the oven. Carbon loading of the microporous layer was measured to be about 2 mg/cm^2 with Teflon loading of about 2 mg/cm^2. This compact microporous layer provides sufficient barrier to methanol transport to the catalyst sites for methanol feed concentrations up to 4–6 M.

A commercial 5 wt.% Nafion solution (EW1100, Aldrich) was modified by diluted sodium hydroxide solution and a viscous organic solvent to make solvent-substituted Nafion solution. This Nafion solution was mixed with unsupported Pt/Ru black (HiSPEC 6000, Pt:Ru = 1:1 atomic ratio, Alfa Aesar) in a nitrogen-protected environment. The resultant solution was spread on the microporous layer using the knife-blade to form the catalyst layer as the anode. After being dried in the nitrogen-filled oven for 30 min, the loadings of Pt/Ru and Nafion in the anode catalyst layer were 4–6 and 1–1.5 mg/cm^2, respectively. To make the cathode catalyst layer, the prepared solution, mixed with the solvent-substituted Nafion solution and carbon-supported Pt (40 wt.% Pt on Vulcan XC72R, E-Tek) in the nitrogen-protected environment, was coated on the microporous layer of the carbon paper also using the knife-blade. Loading of Pt and Nafion in the cathode catalyst layer were 1.3 and 1 mg/cm^2, respectively. The anode and cathode were re-protonated to H$^+$ form of Nafion by using 0.1 M sulfuric acid aqueous solution and then dried again in the oven. Fig. 4 gives two scanning electron micrographs (SEM) of these anode and cathode catalyst layer structures.

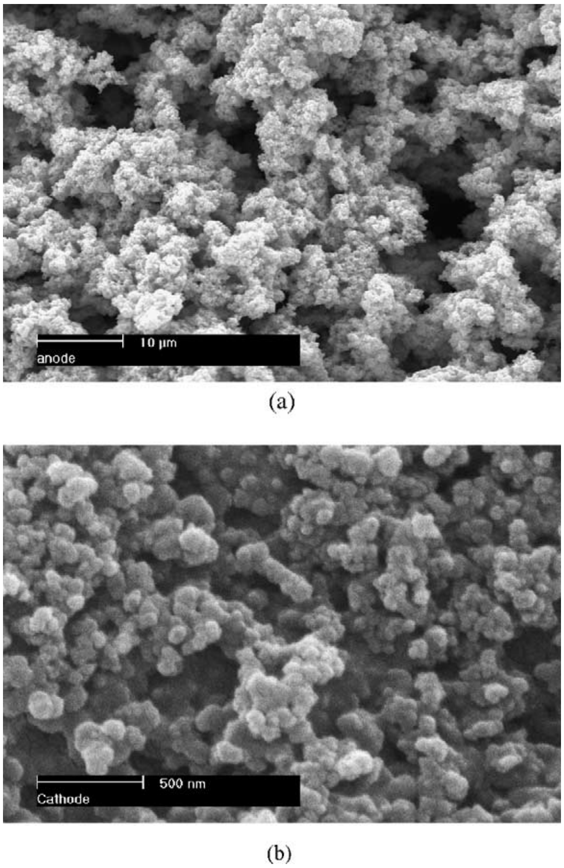

Fig. 4. SEM pictures of the electrodes: (a) anode, and (b) cathode.

Nafion 112 (EW 1100, Dupont) was pretreated by hydrogen peroxide aqueous solution (5 wt.%) at 80 °C for 2 h, followed by immersion in distilled water for 2 h. Then the Nafion 112 was treated with sulfuric acid aqueous solution (1 M) at 80 °C for 2 h, followed by immersion in the distilled water for 2 h. This pretreated Nafion 112 membrane sandwiched by the catalyzed anode and cathode, which were tailored to have the active area of 1.625 cm^2, was hot pressed to form a MEA at 125 °C and 100 kg/cm^2 for 3 min.

2.3. Test apparatus

Methanol aqueous solution was prepared from 1 to 8 M to test the cell performance. A peristaltic pump was used to deliver the liquid fuel and the flow rate was obtained by weighing the fuel delivered per minute. A gas flow meter was used to measure the flow rate of non-preheated and non-humidified air. An electric heater with temperature controller was attached on the surface of the cell to investigate the cell characteristics at different temperatures. An electronic load system (BT4, Arbin) in the galvanodynamic polarization mode was used to measure polarization curve at a scan rate of 3 mA/s. In addition, a Solartron 1287 electrochemical interface together with a Solartron 1260 frequency response analyze were used to measure the cell ohmic resistance.

3. Results and discussion

Due to the deleterious effect of methanol crossover, dilute methanol solutions (i.e. 1 M) were usually used in DMFC. Fig. 5 shows a series of cell polarization curves operated at different temperatures using 1 M methanol solution under the ambient pressure. The flow rate of non-preheated air was 88 ml/min (stoichiometry of 5.32 at a reference current of 0.5 A/cm^2) and the methanol feed rate was 0.283 ml/min (stoichiometry of 3.37 at the reference current of 0.5 A/cm^2). As can be seen from Fig. 5, the polarization curves exhibit kinetic and ohmic control, while the mass transport limitation is not apparent. The impedance measurement of this micro cell at open circuit with a temperature of 60 °C indicated an ohmic resistance of 0.202 Ω cm^2. The maximum power density of the cell reaches 14.27 mW/cm^2 at a voltage of 0.196 V at room temperature (i.e. 23 °C). The maximum power density is 24.75 mW/cm^2 at a voltage of 0.214 V when the temperature increased to 40 °C. This is because the kinetics of electrodes, particularly methanol oxidation at the anode, are enhanced at elevated temperatures. For the same reason, maximum power density is 47.18 mW/cm^2 at a voltage of 0.258 V and temperature of 60 °C. This trend demonstrates that the maximum power density nearly doubles when the cell temperature increases by 20 °C.

Figs. 6 and 7 explore cell performance at different flow rates of air and methanol, respectively, under ambient pressure and temperature of 60 °C using 1 M methanol aqueous solution. Fig. 6 shows the polarization curves as a function of air flow rate when methanol feed rate is fixed at 0.283 ml/min. As the air flow rate increases from 88 ml/min to 161 ml/min, it is seen that the cell performance has no improvement. When the air flow rate reduces to 31 ml/min (stoichiometry of 1.88 at the reference current of 0.5 A/cm^2), the cell performance degrades only a little. Fig. 7 shows the dependence of polarization curves on the methanol feed rate with the air flow rate fixed to 88 ml/min. A mass transport limitation (due to methanol transport in the anode) is clearly seen once the methanol feed rate is reduced to 0.03 ml/min (stoichiometry of 0.36 at the reference current of 0.5 A/cm^2 or 0.18 A/cm^2 equivalent). At this rate, the methanol solution remains almost stationary within the anode channels. Since the channels are shallow (400 μm depth and 750 μm width), carbon dioxide bubbles produced from methanol oxidation cannot be removed efficiently. This results in the liquid channels blocked by gas bubbles, thereby causing the mass transport limitation occurring at 0.125 A/cm^2 on the polarization curve.

The 0.03 ml/min case in Fig. 7 may point to a new design paradigm for micro DMFC. The methanol feed rate in this case is only 0.18 A/cm^2 while the cell current is 0.125 A/cm^2. This leaves a maximum of only 55 mA/cm^2 for methanol crossover assuming that there is no methanol left in the effluent. Clearly, controlling the methanol feed rate can effectively mitigate methanol crossover. As a result, it is seen from Fig. 7 that the cell performance is improved until approaching the mass limiting current density.

For portable application, further improvement of the micro DMFC to simplify cell operation includes air breathing on the cathode side and pumpless delivery of liquid fuel on the anode side. In our recent study, the cell performance

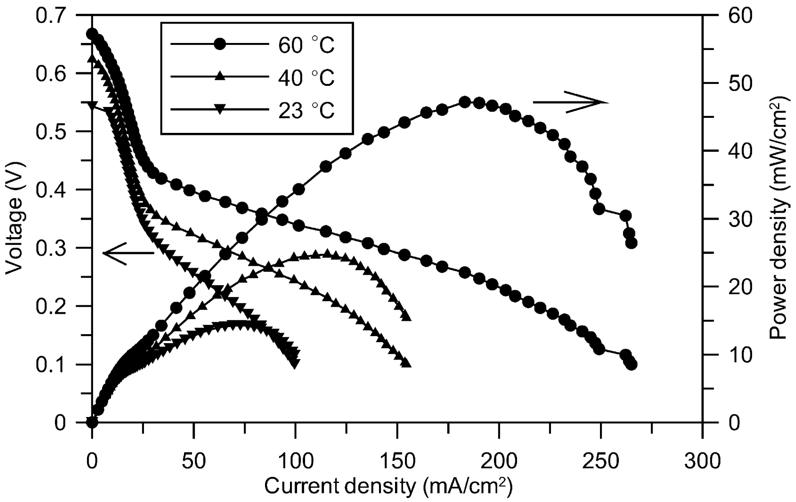

Fig. 5. Polarization and power density curves at different temperatures using 1 M methanol solution with the air flow rate of 88 ml/min and methanol flow rate of 0.283 ml/min at atmospheric pressure.

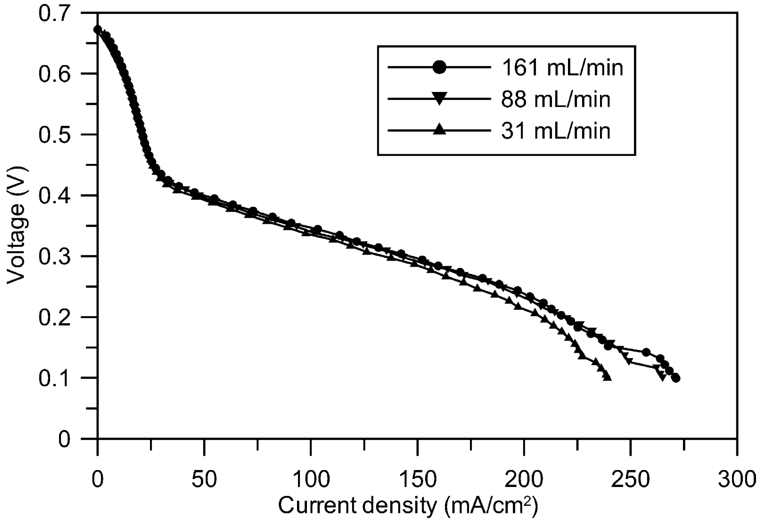

Fig. 6. Polarization curves at different air flow rates using 1 M methanol solution with methanol flow rate of 0.283 ml/min at 60 °C at atmospheric pressure.

did not degrade much in a semi-passive DMFC with an air-breathing cathode but an anode needing a liquid pump for fuel delivery. This finding is consistent with the results given in Fig. 6 where the air flow rate has little effect on cell performance unless the air supply rate becomes exceedingly small. However, Fig. 7 clearly shows that a good circulation of liquid fuel in micro DMFC would be needed to avoid severe mass transport limitation. Thus, it remains challenging to find ways to flow liquid fuel through the cell and to remove carbon dioxide gas efficiently without a parasitic liquid pump.

Fig. 8 displays polarization curves of the micro DMFC for different temperatures under ambient pressure using 2 M methanol solution with feed rates of 88 ml/min on the cathode side and 0.283 ml/min on the anode side. Similar to the cell performance at 1 M methanol solution shown in Fig. 5, significant mass transport limitation is not evident, and the polarization curves are primarily in the kinetic and ohmic control regimes. Compared to Fig. 5 using 1 M methanol solution, Fig. 8 shows that the open circuit voltage drops slightly under 2 M methanol solution due to the methanol crossover effect. The maximum power density of the micro DMFC at 2 M, however, reaches: 50 mW/cm^2 at 0.2 V and 60 °C; 33 mW/cm^2 at 0.17 V and 40 °C; and 16.5 mW/cm^2 at 0.14 V at room temperature.

Figs. 9 and 10 further show the polarization and power density curves for different temperatures under ambient pressure using 4 and 8 M methanol solutions, respectively, with the same feed rates of air and fuel given in Figs. 4 and 8. The methanol crossover rate would become excessive under these highly concentrated methanol solutions at a temperature as high as 60 °C, therefore, no results at this temperature

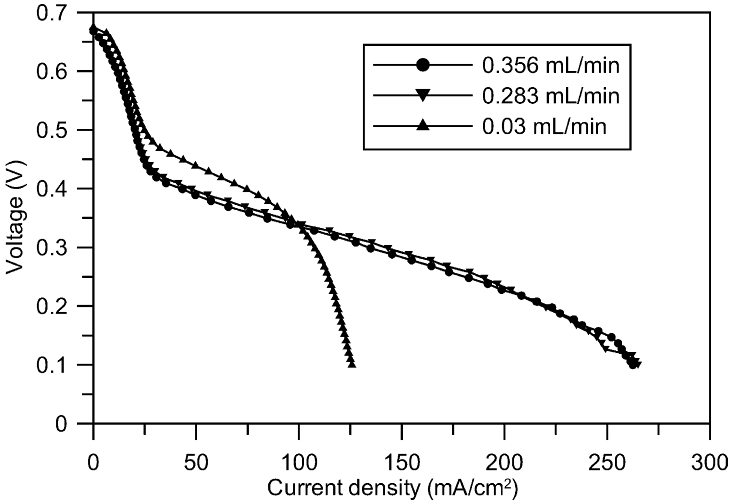

Fig. 7. Polarization curves at different methanol flow rates using 1 M methanol solution with the air flow rate of 88 ml/min at 60 °C at atmospheric pressure.

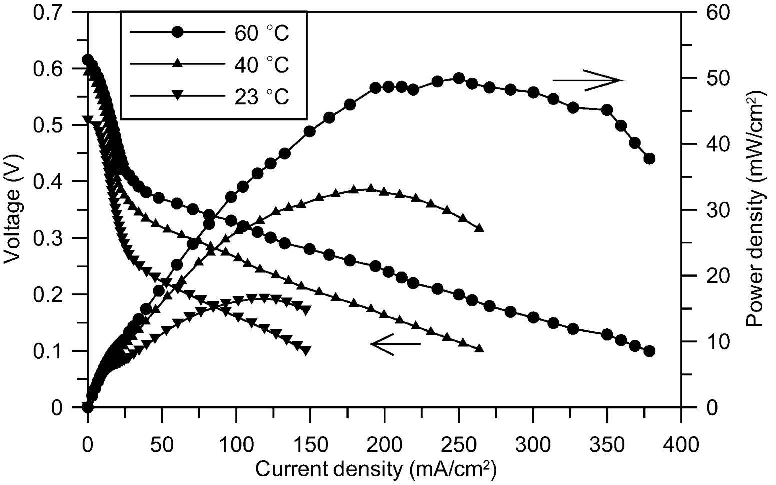

Fig. 8. Polarization and power density curves at different temperatures using 2 M methanol solution with the air flow rate of 88 ml/min and methanol flow rate of 0.283 ml/min at atmospheric pressure.

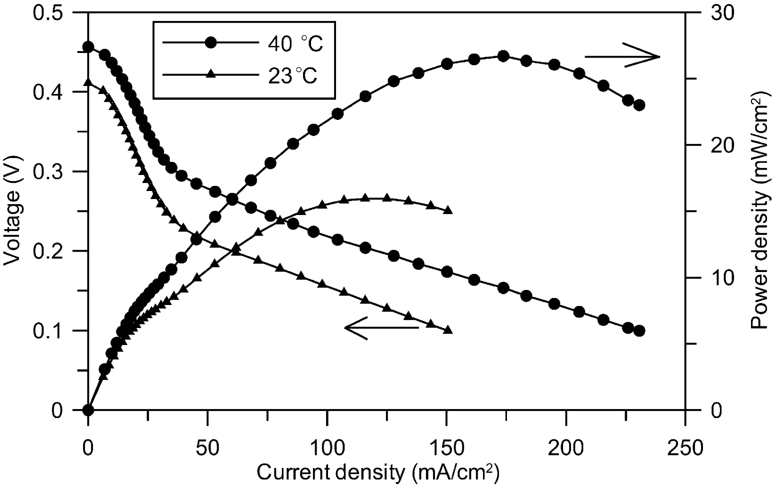

Fig. 9. Polarization and power density curves at different temperatures using 4 M methanol solution with the air flow rate of 88 ml/min and methanol flow rate of 0.283 ml/min at atmospheric pressure.

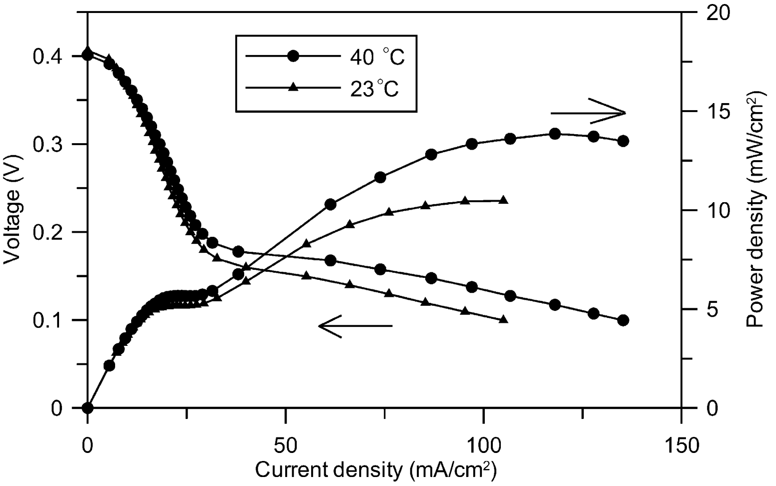

Fig. 10. Polarization and power density curves at different temperatures using 8 M methanol solution with the air flow rate of 88 ml/min and methanol flow rate of 0.283 ml/min at atmospheric pressure.

are shown in Figs. 9 and 10. At near-ambient temperatures (i.e. 40 and 23 °C), the crossover effect is already seen to further reduce the open circuit voltage. But the maximum power density with 4 M methanol solution still reaches 26.7 mW/cm^2 at 0.15 V and 40 °C, and 16 mW/cm^2 at 0.13 V at room temperature, respectively, as can be seen from Fig. 9. This performance with 4 M is comparable to that of 2 M methanol solution. When the feed concentration is 8 M, the maximum power density begins to drop to 13.7 mW/cm^2 at 0.11 V and 40 °C, and 10.5 mW/cm^2 at 0.1 V at room temperature.

Comparing the maximum power densities of the present cell achievable with various concentrations of methanol solution (Figs. 5 and 8–10), it can be seen that 2 and 4 M cases are better; both are higher than 1 M solution as given in Fig. 5 under otherwise identical conditions. The suitability of this MEA for more concentrated fuel stems from the anode backing structure, which consists of a thick carbon paper coated with a compact microporous layer. This backing provides much resistance to methanol transport from the feed into the catalyst sites, thus reducing the amount of crossover. Such a design is so effective that we were able to use Nafion® 112 as the membrane rather than the commonly used Nafion® 117. Our MEA design provides an alternative means to mitigate methanol crossover besides the existing method using thick membranes [16,17].

It is of paramount importance to reduce the size and weight of the fuel tank in micro-power sources. Using 8 M concentrated methanol solution, the fuel tank volume decreases by roughly eight-fold compared to the 1 M dilute solution containing the same amount of pure methanol. Although power density will decrease under concentrated solutions due to methanol crossing over the polymer membrane, the reduction using 8 M solution (10.5 mW/cm^2 at 23 °C) is only 27% as compared to that using 1 M solution (14.3 mW/cm^2 at 23 °C). Therefore, for a micro fuel cell designed to operate at near-room temperatures, it is entirely feasible to use much more concentrated solutions than those addressed in the open literature.

Water balance is another important aspect of DMFC operated with concentrated methanol solution. For each mole of methanol, there is one mole of water needed for methanol oxidation at the anode and 2.5×6 moles of water dragged through the membrane towards the cathode, assuming that the electro-osmotic drag coefficient of water is equal to 2.5 per proton and there is no water back flow through the membrane. This then requires 16:1 molecular ratio for water to methanol, or approximately 3 M. In other words, in a thick membrane like Nafion 117, the maximum molarity at which a DMFC can operate is approximately 3 M. However, in presently designed MEA, the presence of a compact microporous layer permits the use of a much thinner membrane (e.g. N112) without causing excessive methanol crossover, which in turn facilitates water back flow from the cathode to anode, as also demonstrated by Blum et al. [15]. Due to the fact that our MEA is operational in the 8 M methanol solution, the net water transport coefficient through the membrane is estimated to be around 0.6 versus a purely electro-osmotic drag coefficient of 2.5 in thick membranes.

4. Conclusion

A micro direct methanol fuel cell with an active area of 1.625 cm^2 has been developed and its electrochemical properties characterized in this work. MEMS technology has demonstrated capability to provide a fast and flexible venue of fabrication for micro fuel cells with complex flowfield. The micro-fabricated DMFC based on Si wafers, along with a MEA tailored to resist methanol crossover, has demonstrated a maximum power density of about 50 mW/cm^2 at 60 °C and 16.5 mW/cm^2 at room temperature using a 2 M methanol solution under ambient pressure. Moreover, the same cell yielded uncompromising performance at room temperature for methanol feed concentration as high as 4 M, and only slightly degraded performance under a 8 M methanol solution. The combination of high power density, tolerance to concentrated fuel (and thus high energy density), and easy manufacturing makes this type of micro DMFC well suited to power future portable electronics and MEMS devices.

Acknowledgements

This work was supported by DARPA Microsystem Technology Office (MTO) under contract no. DAAH01-1-R001. The first author would also like to acknowledge Fuqiang Liu and Yinghui Pan of ECEC at Penn State University for useful discussions on the experiments.

References

[1] S.R. Narayanan, T.I. Valdez, in: W. Vielstich, A. Lamm, H.A. Gasteiger (Eds.), Handbook of Fuel Cells—Fundamental, Technology and Application, vol. 4, Wiley, New York, 2003, p. 1133.

[2] C.K. Dyer, J. Power Sources 106 (2002) 31.

[3] S.R. Narayanan, H. Frank, B. Jeffries-Nakamura, M. Smart, W. Chun, G. Halpert, J. Kosek, C. Cropley, in: S. Gottesfeld, G. Halpert, A. Landgrebe (Eds.), Proton Conducting Membrane Fuel Cells I, PV 95-23, The Electrochemical Society Proceedings Series, Pennington, NJ, 1995, p. 278.

[4] X. Ren, T.E. Springer, S. Gottesfeld, J. Electrochem. Soc 147 (2000) 92.

[5] A.S. Arico, S. Srinivasan, V. Antonucci, Fuel Cells 1 (2001) 133.

[6] A.K. Shukla, C.L. Jackson, K. Scott, R.K. Raman, Electrochim. Acta 47 (2002) 3401.

[7] M.M. Mench, C.Y. Wang, J. Electrochem. Soc 150 (2003) A79.

[8] S.C. Kelley, G.A. Deluga, W.H. Smyrl, Electrochem. Solid State 3 (2000) 407.

[9] S.C. Kelley, G.A. Deluga, W.H. Smyrl, AICHE J. 48 (2002) 1071.

[10] S.J. Lee, A. Chang-Chien, S.W. Cha, R. O'Hayre, Y.I. Park, Y. Saito, F.B. Prinz, J. Power Sources 112 (2002) 410.

[11] H.L. Maynard, J.P. Meyers, J. Vac. Sci. Technol. B 20 (2002) 1287.

[12] A. Heinzel, C. Hebling, M. Muller, M. Zedda, C. Muller, J. Power Sources 105 (2002) 250.

[13] J.R. Yu, P. Cheng, Z.Q. Ma, B.L. Yi, Electrochim. Acta 48 (2003) 1537.

[14] J. Pavio, J. Bostaph, A. Fisher, J. Hallmark, B.J. Mylan, C.G. Xie, Advancing Microelectron. 29 (2002) 1.

[15] A. Blum, T. Duvdevani, M. Philosoph, N. Rudoy, E. Peled, J. Power Sources 117 (2003) 22.

[16] G.Q. Lu, C.Y. Wang, Electrochemical and Flow Characterization of a Direct Methanol Fuel Cell, Submitted for publication.

[17] C. Lim, C.Y. Wang, J. Power Sources 113 (2003) 145.